Dielectric permittivity profiles of confined polar fluids

V. Ballenegger and J.-P. Hansen
Department of Chemistry, University of Cambridge, Cambridge CB2 1EW, United Kingdom

The dielectric response of a simple model of a polar fluid near neutral interfaces is examined by a combination of linear response theory and extensive molecular dynamics simulations. Fluctuation expressions for a local permittivity tensor $\epsilon(\mathbf{r})$ are derived for planar and spherical geometries, based on the assumption of a purely local relationship between polarization and electric field. While the longitudinal component of ϵ exhibits strong oscillations on the molecular scale near interfaces, the transverse component becomes ill defined and unphysical, indicating nonlocality in the dielectric response. Both components go over to the correct bulk permittivity beyond a few molecular diameters. Upon approaching interfaces from the bulk, the permittivity tends to increase, rather than decrease as commonly assumed, and this behavior is confirmed for a simple model of water near a hydrophobic surface. An unexpected finding of the present analysis is the formation of "electrostatic double layers" signaled by a dramatic overscreening of an externally applied field inside the polar fluid close to an interface. The local electric field is of opposite sign to the external field and of significantly larger amplitude within the first layer of polar molecules. © *2005 American Institute of Physics*. [DOI: 10.1063/1.1845431]

I. INTRODUCTION

The dielectric permittivity of a medium is a macroscopic concept which is defined by the relationship between the polarization **P** and the electric field **E** inside the medium.[1] When the dielectric medium is inhomogeneous over distances much larger than molecular scales, a space-dependent (local) permittivity $\epsilon(\mathbf{r})$ may be defined when dealing with mesoscopic electrostatic problems. The question of how far towards molecular scales a local permittivity remains a meaningful concept, and how $\epsilon(\mathbf{r})$ is related to dipolar fluctuations is a long-standing problem[2] which we have recently addressed in the case of a polar fluid near a sharp interface.[3] We showed that a necessary condition for the existence of a meaningful, statistical definition of a local permittivity is that the local electric field inside the medium does not vary appreciably on the scale of the molecular correlation length, as already noted by Nienhuis and Deutch.[2]

The ability to give a clear-cut statistical definition of a local permittivity is crucial for any coarse-graining strategy, whereby large parts of a complex multicomponent system are treated as continuous dielectric media, while the remaining parts are described in molecular detail. An important example is provided by implicit solvent models of biomolecular assemblies, where water is considered as a continuous dielectric medium, characterized by a local permittivity in the immediate vicinity of biomolecules or membranes. A spatially varying permittivity then determines the electrostatic interactions between charged residues and ions.[4] Conversely one may wish to describe a polar solvent trapped within a dielectric matrix, as in the case of water confined between membranes or clay platelets, or within narrow pores. In these circumstances it may be advantageous to describe the confining matrix as a dielectric continuum, while the confined polar liquid is modeled with molecular resolution.[5]

In this paper we consider the case of polar fluids confined by continuous dielectric media characterized by a permittivity ϵ'. We relate the local dielectric permittivity $\epsilon(\mathbf{r})$ to the dipolar fluctuations within the inhomogeneous fluid, along the lines of the classic Kirkwood–Fröhlich (KF) linear response treatment of the bulk permittivity.[6,7] More specifically, we shall consider the cases of a simple polar fluid in an infinite slab confined by two semi-infinite dielectric media and of a polar fluid confined to a spherical cavity inside a uniform, macroscopic dielectric continuum. Numerical results based on long Molecular Dynamics (MD) simulations will illustrate the limitations of the concept of a local permittivity in the two geometries.

All considerations in this paper will be restricted to sharp interfaces. Like most previous theoretical and numerical work in the field, the present coarse-grained treatment suffers from the inconsistency of ignoring the molecular graininess of the confining media, while using a fully molecular description of the polar fluid.

II. POLARIZATION IN LINEAR RESPONSE

Consider a classical fluid at temperature $T = 1/(k_B \beta)$, made up of N polar molecules carrying dipole moments $\boldsymbol{\mu}_i$, confined to a cavity of arbitrary shape and volume V, carved out of a macroscopic dielectric medium of uniform permittivity ϵ'. The molecules may be polarizable; their interactions are arbitrary at short distances, but tend towards the dipolar interaction at larger distances. The microscopic polarization density is

$$\mathbf{m}(\mathbf{r}) = \sum_{i=1}^{N} \boldsymbol{\mu}_i \delta(\mathbf{r} - \mathbf{r}_i), \qquad (1)$$

where $\mathbf{r}_i$ is the position of the ith molecule inside the cavity. The corresponding total dipole moment is

$$\mathbf{M} = \int_{\mathcal{D}_{\text{cavity}}} \mathbf{m}(\mathbf{r})d\mathbf{r} = \sum_i \boldsymbol{\mu}_i. \qquad (2)$$

Let $\mathbf{P}_0(\mathbf{r}) = \langle \mathbf{m}(\mathbf{r}) \rangle$ be the average local polarization of the fluid in the absence of an externally applied electric field (by definition, $\mathbf{E}'$ is the field far away from the cavity, created by

charges at $|\mathbf{r}| \rightarrow \infty$) $\mathbf{E}'$. In an isotropic phase, $\mathbf{P}_0(\mathbf{r}) = 0$ for points in the bulk of the fluid. Close to the confining boundaries, $\mathbf{P}_0(\mathbf{r})$ is nonzero in general, but may vanish for symmetry reasons, as in the case of linear polar molecules confined in a slab or a spherical cavity (see Sec. III). When a uniform external field is applied to the system, it induces a polarization density defined by

$$\Delta\mathbf{P}(\mathbf{r}) = \mathbf{P}(\mathbf{r}) - \mathbf{P}_0(\mathbf{r}) = \langle \mathbf{m}(\mathbf{r}) \rangle_{\mathbf{E}'} - \langle \mathbf{m}(\mathbf{r}) \rangle = \frac{\int [\mathbf{m}(\mathbf{r}) - \langle \mathbf{m}(\mathbf{r}) \rangle] \exp[-\beta(U_{\epsilon'}(1,\ldots,N) - \mathbf{M} \cdot \mathbf{E}_{\text{c}})]d1\cdots dN}{\int \exp[-\beta(U_{\epsilon'}(1,\ldots,N) - \mathbf{M} \cdot \mathbf{E}_{\text{c}})]d1\cdots dN}, \qquad (3)$$

where we have used the short-hand notation i for the degrees of freedom of the ith molecule. For linear nonpolarizable molecules, $i = (\mathbf{r}_i, \boldsymbol{\mu}_i)$ reduces to the position and orientation of the permanent dipole moment, and integration with phase space element $di = d^3\mathbf{r}_i d\Omega_{\boldsymbol{\mu}_i}$ is performed over all possible positions and orientations of the molecule inside the cavity. $U_{\epsilon'}$ is the total interaction energy of the N polar molecules of the fluid within the cavity in the absence of $\mathbf{E}'$; it depends obviously on the permittivity ϵ' of the surrounding dielectric. The instantaneous total dipole moment $\mathbf{M}$ couples to the cavity field $\mathbf{E}_{\text{c}}$, i.e., the electric field inside the cavity in the absence of polar fluid, when the external (applied) field in the embedding dielectric is $\mathbf{E}'$. The two fields are related by the usual boundary conditions of macroscopic electrostatics.

Let $\Delta\mathbf{E}(\mathbf{r}) = \mathbf{E}(\mathbf{r}) - \mathbf{E}_0(\mathbf{r})$ be the difference between the mean local electric field inside the cavity, due to the external field and all the dipoles, and the mean electric field when no external field is applied [note that $\mathbf{E}_0(\mathbf{r}) = 0$ if $\mathbf{P}_0(\mathbf{r}) = 0$ everywhere]. Then, within the linear regime [i.e., for not too strong $\Delta\mathbf{E}(\mathbf{r})$], the induced polarization density is related to $\Delta\mathbf{E}(\mathbf{r})$ via

$$\Delta\mathbf{P}(\mathbf{r}) = \frac{1}{4\pi} \int_{\mathcal{D}_{\text{cavity}}} \underline{\chi}(\mathbf{r},\mathbf{r}') \cdot \Delta\mathbf{E}(\mathbf{r}')d\mathbf{r}', \qquad (4)$$

where $\underline{\chi}$ is the dielectric susceptibility tensor. In the slow modulation limit, i.e., for slowly varying $\Delta\mathbf{E}(\mathbf{r})$, the integral factorizes approximately, and Eq. (4) reduces to the local form

$$\Delta\mathbf{P}(\mathbf{r}) = \frac{1}{4\pi}\underline{\chi}(\mathbf{r}) \cdot \Delta\mathbf{E}(\mathbf{r}), \qquad (5)$$

where, formally, $\underline{\chi}(\mathbf{r},\mathbf{r}') = \underline{\chi}(\mathbf{r})\delta(\mathbf{r}-\mathbf{r}')$. The local permittivity tensor is defined by

$$\underline{\chi}(\mathbf{r}) = \underline{\epsilon}(\mathbf{r}) - \underline{I}. \qquad (6)$$

Linearization of Eq. (3) with respect of $\mathbf{E}_{\text{c}}$ leads to the following relation between the components of $\Delta\mathbf{P}(\mathbf{r})$ and $\mathbf{E}_{\text{c}}(\mathbf{r})$:

$$\Delta P_\alpha(\mathbf{r}) = \beta \sum_{\gamma=x,y,z} [\langle m_\alpha(\mathbf{r})M_\gamma \rangle - \langle m_\alpha(\mathbf{r}) \rangle \langle M_\gamma \rangle] E_\gamma^c, \qquad (7)$$

where $\alpha, \gamma = x$, y, or z and the statistical averages are understood to be taken at zero external (and hence cavity) field, i.e., with a Boltzmann weight $\exp(-\beta U_{\epsilon'})$. As expected for the linear response to a uniform external field, Eq. (7) involves the average correlation between a fluctuation in the local polarization density $\mathbf{m}(\mathbf{r})$ and a fluctuation in the global dipole moment $\mathbf{M}$ of the system, as has been recognized recently by Stern and Feller.[8] Note that $\langle \mathbf{M} \rangle$ will be zero by symmetry in all systems we shall consider.

Comparison between Eqs. (5) and (7) does not provide a fluctuation formula for $\chi(\mathbf{r})$ or $\epsilon(\mathbf{r})$, since they involve the total and cavity fields, respectively. The relation between these two fields depends on the geometry of the cavity, and can be established within macroscopic electrostatics. We consider successively the case of slab and spherical geometries.

A. Slab geometry

We consider a cavity in the form of an infinite slab where a fluid of $\rho = N/V$ polar molecules per unit volume is confined in the z direction by two infinite dielectric walls of permittivity ϵ'. The distance between the dielectric walls is L. The confined fluid is inhomogeneous in the z direction (orthogonal to the walls) only. By symmetry, the permittivity tensor reduces to the diagonal form

$$\epsilon(z) = \begin{pmatrix} \epsilon_\parallel(z) & 0 & 0 \\ 0 & \epsilon_\parallel(z) & 0 \\ 0 & 0 & \epsilon_\perp(z) \end{pmatrix}, \qquad (8)$$

where $\epsilon_\parallel$ and $\epsilon_\perp$ denote the components parallel and orthogonal to the walls. Equations (5) and (6) then combine into two independent relations,

$$\mathbf{P}_\parallel(z) = \frac{\epsilon_\parallel(z) - 1}{4\pi} \mathbf{E}_\parallel(z), \qquad (9a)$$

$$\Delta\mathbf{P}_\perp(z) = \frac{\epsilon_\perp(z)-1}{4\pi}\Delta\mathbf{E}_\perp(z). \tag{9b}$$

We dropped the symbol Δ in Eq. (9a) because isotropy in the (x,y)-plane implies that $\mathbf{P}_0(\mathbf{r})$ (the average polarization in the absence of external field) has no parallel components. Using the standard boundary conditions on the normal and tangential components of the electric field, one finds the following relations between the components of the uniform external field $\mathbf{E}'$ and the cavity field $\mathbf{E}_c$,

$$\mathbf{E}_\parallel^c = \mathbf{E}_\parallel', \quad E_\perp^c = \epsilon' E_\perp', \tag{10}$$

where $E_\perp^c$ and $E_\parallel'$ are two-dimensional vectors in the (x,y) plane; the orthogonal components are along the z direction. Maxwell's equation $\nabla\times\mathbf{E}(z)=0$ implies

$$\frac{\partial E_x(z)}{\partial z} = \frac{\partial E_y(z)}{\partial z} = 0, \tag{11}$$

so that $\mathbf{E}_\parallel = (E_x, E_y)$ is independent of z, i.e., $\mathbf{E}_\parallel(z) = E_\parallel'$ everywhere in space. In other words, Eq. (9a) leads to

$$\mathbf{P}_\parallel(z) = \frac{\epsilon_\parallel(z)-1}{4\pi}\mathbf{E}_\parallel' = \frac{\epsilon_\parallel(z)-1}{4\pi}\mathbf{E}_\parallel^c. \tag{12}$$

Comparison of Eqs. (7) and (12), together with isotropy in the (x,y) plane then leads to the desired fluctuation formula for $\epsilon_\parallel(z)$:

$$\epsilon_\parallel(z) = 1 + 2\pi\beta[\langle\mathbf{m}_\parallel(z)\cdot\mathbf{M}_\parallel\rangle - \langle\mathbf{m}_\parallel(z)\rangle\cdot\langle\mathbf{M}_\parallel\rangle]. \tag{13}$$

The orthogonal component may be determined from Maxwell's equation $\nabla\cdot\mathbf{D}(z)=0$, where $\mathbf{D}=\mathbf{E}+4\pi\mathbf{P}$ is the displacement vector, leading to

$$\frac{\mathrm{d}}{\mathrm{d}z}[E_\perp(z) + 4\pi P_\perp(z)] = 0. \tag{14}$$

Integration of Eq. (14) from $-\infty$ to z yield

$$E_\perp(z) - E_\perp' = -4\pi P_\perp(z) + 4\pi P_\perp(z=-\infty)$$

$$= -4\pi P_\perp(z) + (\epsilon'-1)E_\perp'. \tag{15}$$

Substracting from Eq. (15) the same equation without external field and using Eq. (9b) gives $\epsilon_\perp(z)\Delta E_\perp(z) = \epsilon' E_\perp' = E_\perp^c$, where the second equality follows from Eq. (10). Equation (9b) may hence be rewritten as

$$P_\perp(z) = \frac{1}{4\pi}\frac{\epsilon_\perp(z)-1}{\epsilon_\perp(z)}E_\perp^c. \tag{16}$$

Comparison of Eq. (16) with the transverse ($\alpha=\perp$) version of Eq. (7) leads to the desired fluctuation formula for $\epsilon_\perp(z)$,

$$\frac{\epsilon_\perp(z)-1}{\epsilon_\perp(z)} = 4\pi\beta[\langle m_\perp(z)M_\perp\rangle - \langle m_\perp(z)\rangle\langle M_\perp\rangle]. \tag{17}$$

Equations (13) and (17) are the appropriate fluctuation formulas to compute the permittivity tensor $\epsilon(z)$ of a system inhomogeneous in one direction. Note that these formulas depend only implicitly, via the statistical averages weighted by the Bolzmann factor $\exp(-\beta U_{\epsilon'})$, on the permittivity ϵ' of the confining medium. This is to be contrasted with the results for spherical samples to be discussed below.

The key finding is that a local expression of the permittivity involves correlations of the local and total polarization of the form $\langle m_\alpha(z)M_\gamma\rangle$, and not of the local polarization alone, as has sometimes been wrongly assumed in the literature. This was already recognized by Stern and Feller,[8] but their expression for the permittivity tensor $\epsilon(z)$ differs from the one derived here, because they did not consider a single slab, but a system which is periodically replicated in space to form an infinite spherical array of the original slab.

We stress that formulas (13) and (17) were derived for a uniform external field under the local assumption (5). If the local assumption is not valid, definitions (9a) and (9b) become purely formal, and the permittivity $\epsilon(z)$ may take values that are unphysical and specific to the case of a uniform external field permeating a planar interface.

B. Spherical geometry

We now consider a system of N polar molecules confined to a spherical cavity of radius R, surrounded by a dielectric medium of permittivity ϵ'. We first recall the fluctuation formula for the *bulk* dielectric constant of this system. The cavity field is now $\mathbf{E}^c = 3\epsilon'\mathbf{E}'/(2\epsilon'+1)$. For a macroscopic spherical sample of uniform permittivity ϵ, the local field, far from the boundaries, is uniform and equal to $\mathbf{E} = 3\epsilon'\mathbf{E}'/(2\epsilon'+\epsilon)$. Substituting $\mathbf{E}^c$ and $\mathbf{E}$ into Eq. (7) and into the definition (5) of the polarization, one arrives, upon identification and use of the isotropy of the system, at

$$\frac{(\epsilon-1)(2\epsilon'+1)}{(2\epsilon'+\epsilon)} = \frac{4\pi\epsilon}{3}[\langle\mathbf{m}(\mathbf{r})\cdot\mathbf{M}\rangle - \langle\mathbf{m}(\mathbf{r})\rangle\cdot\langle\mathbf{M}\rangle]. \tag{18}$$

In this formula $\mathbf{r}$ can be any point in the bulk of the sample, so that $\mathbf{m}(\mathbf{r})$ may be replaced by $\mathbf{M}/V$ if boundary effects are negligible. This leads back to the well known KF formula for the bulk dielectric constant in terms of fluctuations ($\langle\mathbf{M}^2\rangle - \langle\mathbf{M}\rangle^2)/V$ of the total dipole moment of the system.[7] Since boundary conditions in computer simulations are designed to minimize finite size effects, the KF formula can be used, as expected, to compute the dielectric constant in a simulation performed with a reaction field or periodic boundary conditions (if the Ewald sums are performed using the spherical convention for the order of summation).[9] For a confined spherical system which is *not* periodically repeated, the dielectric constant should be computed from Eq. (18) (see Sec. III B).

Attempts have been made to generalize the KF relation, valid for a macroscopic spherical system, to mesoscopic samples, where $\mathbf{P}(\mathbf{r})$, $\mathbf{E}(\mathbf{r})$, and the resulting $\epsilon(\mathbf{r})$ are nonuniform near the confining surface.[10,11] Strictly speaking, $\epsilon(\mathbf{r})$ is, however, no longer a scalar near the sample boundary, but a tensor with radial and tangential components.

We consider here the case where the external field is radial, preserving thus the spherical symmetry of the problem. Such a radial field can arise from an external charge q placed at the center of the spherical cavity filled with polar molecules, or polar residues of a globular macromolecule (e.g., a protein); in that case the nonuniform external field is $\mathbf{E}'(\mathbf{r}) = (q/r^2)\hat{\mathbf{r}}$ where $\hat{\mathbf{r}} = \mathbf{r}/r$. The dipoles of the confined fluid or macromolecule couple to this field with energy,

$$U_{\text{ext}} = -\sum_i \boldsymbol{\mu}_i \cdot \mathbf{E}'(\mathbf{r}) = -\int_{\mathcal{D}_{\text{cavity}}} m(\mathbf{r})E'(\mathbf{r})d\mathbf{r}, \qquad (19)$$

where $m(\mathbf{r}) = \mathbf{m}(\mathbf{r}) \cdot \hat{\mathbf{r}}$ is the radial component of the microscopic polarization density (1), and $E'(r) = q/r^2$. Substituting (19) into the Boltzmann factor in the definition (3) of the polarization, and linearizing (which is valid in the limit of small q), one arrives at the following relation between the radial component of $\mathbf{P}(\mathbf{r})$ and the radial component of the external field:

$$P(r) = \mathbf{P}(\mathbf{r}) \cdot \hat{\mathbf{r}} = \langle m(\mathbf{r}) \rangle + \beta \int_{\mathcal{D}_{\text{cavity}}} d\mathbf{r}' [\langle m(\mathbf{r})m(\mathbf{r}') \rangle$$
$$- \langle m(\mathbf{r}) \rangle \langle m(\mathbf{r}') \rangle] E'(\mathbf{r}'), \qquad (20)$$

where the statistical averages are once more taken at zero external field. We consider the case of molecules carrying linear dipoles, so that $\langle m(\mathbf{r}) \rangle = 0$ by symmetry. We now assume a local relationship between $P(\mathbf{r})$ and the radial local field $E(\mathbf{r})$ in the general form defined by Eqs. (5) and (6), and involving a local dielectric permittivity $\epsilon(r)$,

$$P(r) = \frac{\epsilon(r) - 1}{4\pi} E(r). \qquad (21)$$

This relationship, together with $\nabla \cdot \mathbf{D}(\mathbf{r}) = 4\pi q \delta(\mathbf{r})$, implies that the fields $E(r)$ and $E'(r)$ are related by

$$E(r) = \frac{E'(r)}{\epsilon(r)}. \qquad (22)$$

Combination of Eqs. (20), (21), and (22) then leads to the following relation for $\epsilon(r)$:

$$\frac{1}{4\pi} \frac{\epsilon(r) - 1}{\epsilon(r)} E'(r) = \beta \int_{\mathcal{D}_{\text{cavity}}} d\mathbf{r}' \langle m(\mathbf{r})m(\mathbf{r}') \rangle E'(r') \quad (23)$$

or, substituting $E'(r) = q/r^2$,

$$\frac{\epsilon(r) - 1}{\epsilon(r)} = 4\pi\beta \int_{\mathcal{D}_{\text{cavity}}} d\mathbf{r}' \langle m(\mathbf{r})m(\mathbf{r}') \rangle \left(\frac{r}{r'}\right)^2. \qquad (24)$$

Note that, contrary to Eq. (18), this relation does not depend explicitly on the permittivity ϵ' of the confining medium. The present space-dependent dielectric constant $\epsilon(r)$ describes the screening by the polar fluid of the external field created by the point charge q, as is obvious from Eq. (22). It reduces to the bulk dielectric constant when r is sufficiently large, but still small compared to the radius R of the spherical cavity.

III. MOLECULAR DYNAMICS RESULTS

A. Slab geometry

We have carried out a number of long MD simulations (spanning tens of nanoseconds) to obtain estimates of $\epsilon_{\parallel}(z)$ and $\epsilon_{\perp}(z)$ from the fluctuation formulas (13) and (17). In a slab of width L, 3500 dipolar soft spheres (DSS) were placed. The confining walls at $z=0$ and $z=L$ are assumed to be nonpolarizable ($\epsilon'=1$). The simulation cell is a cube with edges of length L, and periodic boundary conditions are imposed in the (x,y) directions. Each molecule carries an ex-

tended dipole $\boldsymbol{\mu}$ made up of two opposite charges $\pm q$ placed at $\pm\mathbf{d}/2$ from the center, such that $\mu=qd$; the elongation was chosen to be $d/\sigma=1/3$, where σ is the molecular diameter. The bulk dielectric behavior of fluids with such extended dipoles has been shown to be very similar to that of fluids with point dipoles, as long as $d/\sigma < 1/2$.[12] The short-range repulsion between the spherical molecules is chosen to be of the "soft sphere" form

$$u_{\text{Sr}}(r) = 4u \left(\frac{\sigma}{r}\right)^{12} \qquad (25)$$

with $\sigma = 0.366$ nm and $u = 1.85$ kJ/mole [the charges $\pm q$ carry a mass $m=5$ amu; a molecule has hence a total mass of $2m$ and a reduced moment of inertia $I^* = I/2m\sigma^2 = 1/9$. The simulations were performed with the simulation package GROMACS.[13] The equations of motion were integrated with a time step $dt=2$ fs (reduced time step $dt^* = dt/(m\sigma^2/u)^{1/2} = 0.0024$)]. The walls exert a force on the center of mass of the molecules that derives from the potential,

$$U_{\text{walls}}(z) = \frac{4\pi u}{45} \left[\frac{\sigma^9}{z^9} + \frac{\sigma^9}{(L-z)^9}\right]. \qquad (26)$$

This potential follows from integrating the soft-sphere repulsion potential (25) over the regions $z<0$ and $z>L$, for a wall of density $\rho_{\text{wall}}\sigma^3 = 1$. The long range Coulomb interactions between the charges $\pm q$ and the infinite array of periodic images are computed by a slab-adapted version of the usual 3D Ewald summation, as explained in the Appendix.

The structure of the fluid inside the slab is best characterized by the density-orientation profile $\rho(z,\theta)$, where θ is the angle between a molecular dipole and the z axis. This may be expanded in Legendre polynomials according to

$$\rho(z,\theta) = \sum_{\ell=0}^{\infty} \rho_\ell(z) P_\ell(\cos \theta), \qquad (27)$$

where $\rho_\ell(z) = 1/2(2\ell+1)\int_{-1}^{+1}\rho(z,\theta)P_\ell(\cos\theta)d(\cos\theta)$. In the case of uncharged walls, only even coefficients appear in the series (27) because of the symmetry $\rho(z,\theta) = \rho(z,\pi-\theta)$. The $\ell=0$ coefficient $\rho_0(z) = \rho(z)/2$ is one half of the density profile $\rho(z) = \int_0^\pi \rho(z,\theta)\sin\theta d\theta$. The ratio

$$\alpha(z) = \frac{\rho_{\ell=2}(z)}{\rho(z)} \qquad (28)$$

provides a measure of the mean alignment of the dipoles. Since $P_2(x) = (3x^2-1)/2$, $\alpha(z)$ is negative if the dipoles are predominantly aligned parallel to the interface [$\alpha(z) = -5/4$ for complete alignment], while $\alpha(z)$ is positive for predominantly orthogonal alignment [$\alpha(z) = 5/2$ for full alignment orthogonal to the interface].

We performed the simulations at a constant temperature $T = 300$ K (reduced temperature $T^* = kT/u = 1.35$), and for two values of the dipole moment: $\mu = 1.47$ and 2.45 D, corresponding to a reduced dipole $\mu^* = \sqrt{\mu^2/\sigma^3 u} = 1.2$ and 2, respectively. The width of the slab was adjusted to $L = 16.62\sigma$, so that the reduced density of the fluid far from the walls is $\rho^*_{\text{bulk}} = \rho_{\text{bulk}}\sigma^3 = 0.8$. The bulk dielectric constant of this polar fluid is 98 ± 2 at $\mu^* = 2$,[12,14] and about 10 at $\mu^* = 1.2$.
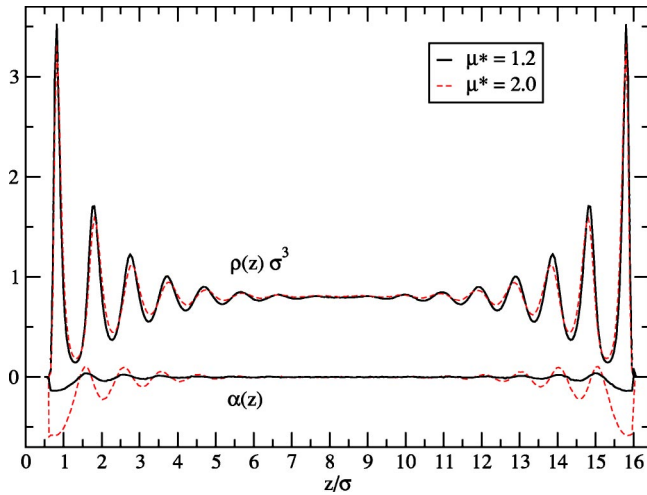
FIG. 1. Density and orientational profile of a DSS fluid in a slab ($T^* = 1.35$, $\rho^*_{\mathrm{bulk}} = 0.8$) for two values of the reduced dipole moment.

FIG. 2. Parallel component of the permittivity tensor (same system as in Fig. 1), from fluctuation formula (13) and from the response to an external field $E' = 0.1$ V/nm along x axis.

The resulting density and orientation profiles $\rho(z)$ and $\alpha(z)$ in zero applied field are plotted in Fig. 1. Layering along the walls occurs in an interfacial region of five to six molecular diameters. The first layer of molecules is seen to align its dipoles parallel to the interface, but orientational ordering is rapidly lost further away from the dielectric walls. The ordering of molecular dipoles parallel to the wall in the first layer may be understood qualitatively in terms of electrostatic interactions of these dipoles with their images.[15] Strictly speaking, there are no images on the molecular scale since the walls are not polarizable, but image charge interactions arise on the mesoscopic scale because of the dielectric discontinuity between the polar fluid ($\epsilon > 1$) and the walls ($\epsilon' = 1$). The behavior of the density-orientation profile far from a single dielectric wall has been studied by Badiali, who showed that $\rho(z)$ is given asymptotically by its bulk value plus an A/z^3 tail arising from the dielectric discontinuity between ϵ and ϵ'.[16]

Parallel and perpendicular permittivity profiles $\epsilon_\|(z)$ and $\epsilon_\perp(z)$ were estimated from the simulations in zero external field using the fluctuation formulas (13) and (17), as well as from simulations in the presence of an external field, by evaluation of the ratio $P(z)/E(z)$ of the induced local polarization and electric field [cf. Eqs. (9)].

Results for the parallel permittivity $\epsilon_\|(z)$ obtained by both routes are shown in Fig. 2 (the simulation with $E' = 0$ lasted 28 ns, while that with $E' = 0.1$ V/nm along the x axis was 3.5 ns long). The agreement between the two independent estimates is seen to be perfect. The pronounced oscillations of $\epsilon_\|(z)$ near the walls closely mirror the oscillations in the density profile apparent in Fig. 1. In fact the ratio $\epsilon_\|(z)\rho_{\mathrm{bulk}}/\rho(z)$, also shown in Fig. 2, shows much less structure. Towards the middle of the slab, $\epsilon(z)$ is seen to be constant and to take a value $\epsilon \simeq 10$ (for $\mu^* = 1.2$) and $\epsilon \simeq 96$ (for $\mu^* = 2$), in agreement with the bulk value derived from MD simulations of a periodic nonconfined fluid at the same state point. Note that on average, $\epsilon_\|(z)$ tends to increase above its bulk value close to the confining walls; in other words, parallel dipolar fluctuations tend to be enhanced near a dielectric
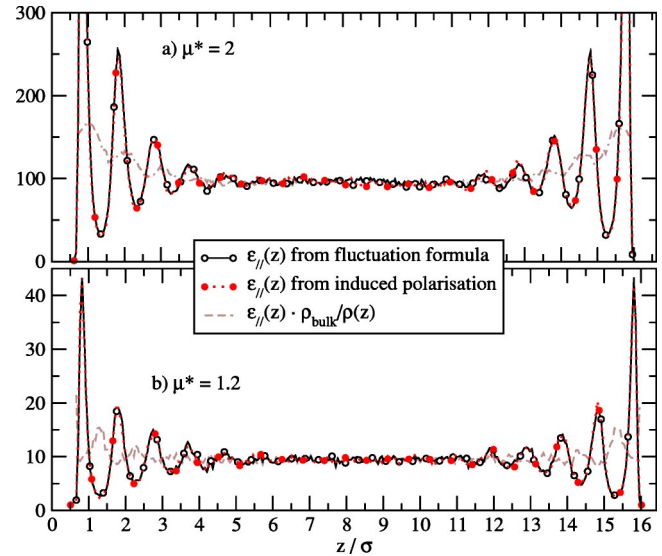
wall with $\epsilon' = 1$. This is contrary to the prediction of a generalization of the familiar Onsager cavity model to the case of a dipolar fluid near a dielectric wall.[17]

Turning to the perpendicular permittivity $\epsilon_\perp(z)$, we consider first the MD results obtained in the absence of external field. The structure of the fluctuation formula (17) is very unfavorable for the estimation of large values of the permittivity since the ratio of the left-hand side is then close to 1, so that statistical uncertainties on the fluctuation expression on the right-hand side, which we shall henceforth denote by $f(z)$, will be dramatically amplified on the quantity of interest $\epsilon_\perp(z) = 1/[1 - f(z)]$. This shortcoming is illustrated in Fig. 3 for the case $\mu^* = 1.2$ (we did not succeed in extracting $\epsilon_\perp(z)$ from dipolar fluctuations in the case $\mu^* = 2$). The signal $f(z)$ calculated by dividing the slab width L into 300 "bins" is seen to be rather noisy, despite the length of the simulation (28 ns). The fluctuations are strongly enhanced near the
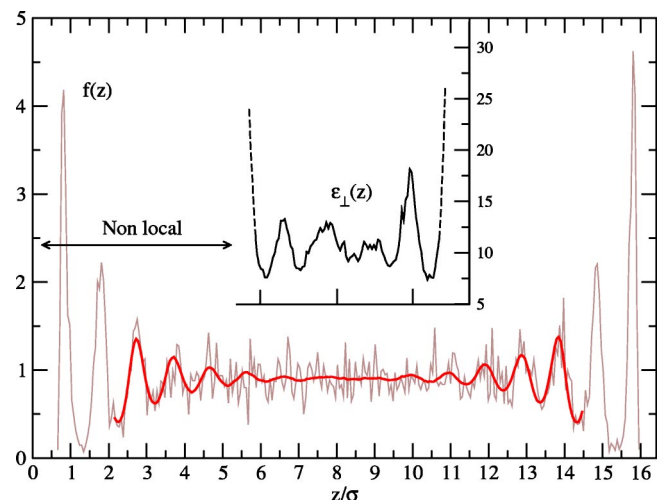
FIG. 3. Dipolar fluctuations $f(z)$ (thin line) and smoothed curve $\bar{f}(z)$ (thick line) [see text]. Inset: orthogonal component of the permittivity tensor ($\mu^* = 1.2$, $T^* = 1.35$, $\rho^*_{\mathrm{bulk}} = 0.8$).
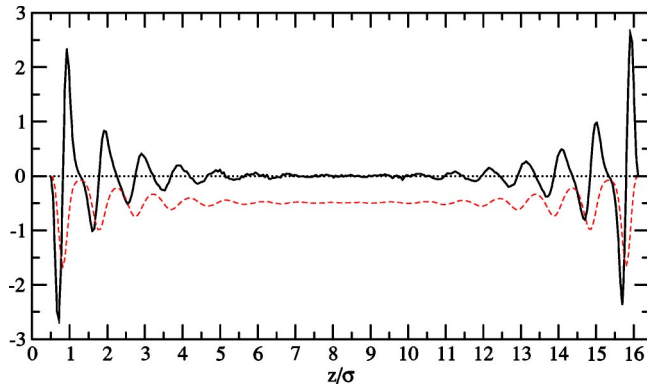
FIG. 4. Continuous line: polarization charge density $c(z)$ $[e/nm^3]$ induced inside a slab of polar fluid ($\mu^* = 1.2$, $\rho^*_{bulk} = 0.8$, $T^* = 1.35$) by an external electric field $E' = 1$ V/nm along the z direction. Dashed line: ten times the integral $\int_0^z c(z')dz'$.

walls, but these values lead to nonphysical, negative values of $\epsilon_\perp(z)$, pointing to the inadequacy of the local assumption (9). A smoothed curve $\bar{f}(z)$ is obtained by averaging the signal $f(z)/\rho(z)$ over intervals of width 3σ, and multiplying the result by the local density $\rho(z)$. The resulting estimate of $\epsilon_\perp(z)$ in the central region of the slab is shown in the inset of Fig. 3.

The statistical uncertainties are still large, but the average value is compatible with a bulk permittivity $\epsilon_\perp = \epsilon_\parallel \simeq 10$. Outside this central "bulk" interval, $\epsilon_\perp(z)$ becomes unphysical whenever $f(z)$ exceeds 1.

We have investigated the transverse dielectric response by applying an external field $E' = 1$ V/nm along the z axis of the moderately polar fluid ($\mu^* = 1.2$, simulation time: 12 ns). This large value was chosen such that the local (screened) field near the center of the slab, $E(z) = E'/\epsilon_\perp(z)$, is still sufficiently strong to induce a sizeable polarization. The local charge density $c(z)$ induced by the applied field is plotted in Fig. 4. As expected it is antisymmetric with respect to midplane ($z = L/2$), and integration of $c(z)$ over the left-hand and right-hand halves of the slab leads to induced surface charge densities $c_S \simeq \pm 0.05$ e/nm^2. The local electric field $E(z)$ is calculated from

$$E(z) = E' + 4\pi \int_0^z c(z')dz' \qquad (29)$$

and the polarization density may then be deduced from

$$P(z) = \frac{E' - E(z)}{4\pi} = -\int_0^z c(z')dz' \qquad (30)$$

while the permittivity profile follows from

$$\epsilon_\perp(z) = \frac{E'}{E(z)}. \qquad (31)$$

Results obtained in this way for $E(z)$, $P(z)$, and $\epsilon_\perp(z)$ are plotted in Fig. 5. The polarization profile $P(z)$ can also be determined from the statistical average $\langle m(z) \rangle$ of the microscopic polarization density alone (dotted line in Fig. 5). The local electric field $E(z)$ exhibits large oscillations close to the walls. Inside the first layer, $E(z)$ is strongly negative
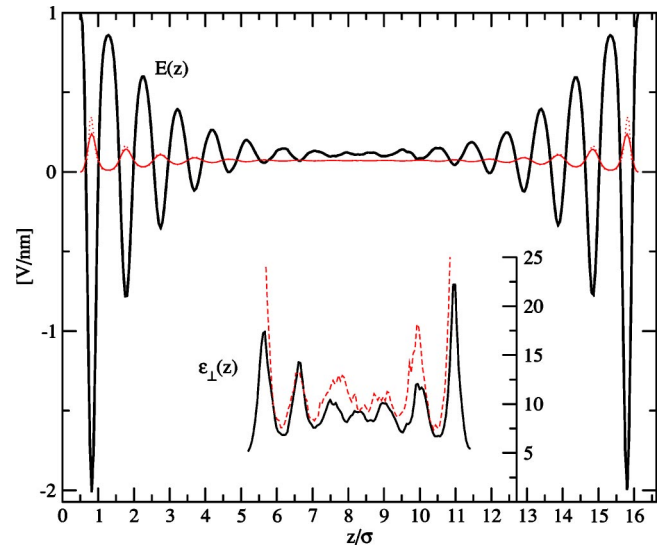
FIG. 5. Electric field $E(z)$ (thick line) and polarization density $P(z)$ computed using Eq. (30) (thin line) and from the statistical average $\langle m(z) \rangle$ (dotted line), for the same system as in Fig. 4. Inset: $\epsilon_\perp(z)$ from Eq. (31) and from fluctuation formula (17) (dashed line).

($\simeq -2$ V/nm), i.e., the external field E' is *overscreened* by a factor of 2! We refer to this remarkable effect as the formation of an "electrostatic double layer" (EDL). Beyond the first layer, the oscillations in $E(z)$ are gradually damped, but are still visible in the central part of the slab, where the oscillations are around a mean value of about 0.1 V/nm. The polarization $P(z)$ oscillates out of phase with $E(z)$ as expected, and the two estimates, based on Eq. (30) and on $\langle m(z) \rangle_{E'}$, are in excellent agreement. So are the estimates of $\epsilon_\perp(z)$ based on Eqs. (17) and (31), despite the large statistical uncertainties. As pointed out above, the relation between $P_\perp(z)$ and $E_\perp(z)$ is nonlocal [i.e., of the more general form (4)] near the walls, where $\epsilon(z) = 1 + 4\pi P(z)/E(z)$ can take negative values, and diverges whenever $E(z) = 0$. Hence $\epsilon_\perp(z)$ is not a useful quantity near the walls. A more relevant quantity is the normalized EDL profile $E(z)/E'$. For weak fields, it is given by linear response theory, viz.,

$$\frac{E_\perp(z)}{E'} = 1 - 4\pi\beta[\langle m_\perp(z)M_\perp \rangle - \langle m_\perp(z) \rangle \langle M_\perp \rangle]$$

$$= 1 - f(z). \qquad (32)$$

Figure 6 illustrates the good agreement between the EDL profiles computed from the fluctuations $f(z)$ (properly smoothed as in Fig. 3) and directly from the ratio $E_\perp(z)/E'$. The small discrepancies close to the walls are probably due to the fact that the extended dipoles are treated as point dipoles in the evaluation of $f(z)$. In order to investigate the influence of the dipole extension d/σ on the striking overscreening effect observed in the EDL profile near the walls, we have also carried out simulations for an extension $d/\sigma = 0.1$ (compared to 0.3 in the previous simulations), keeping the dipole moment fixed at $\mu^* = 1.2$. An oscillatory profile of $E(z)$ similar to that in Fig. 5 is once more observed, but the amplitude of the oscillation closest to the two walls increases by $\approx 50\%$ (from -2 to about -3 V/nm), thus pointing to an
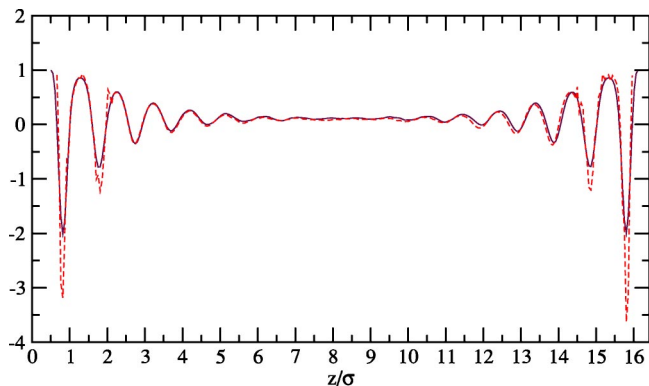
FIG. 6. EDL ratio $E_\perp(z)/E'$ from Eq. (29) (continuous line) and from the fluctuation formula (32) (dashed line) [same system as in Fig. 3].

enhancement of the overscreening effect as the point dipole limit is approached.

We also carried out one long (30 ns) MD run of 2076 SPC water molecules,[18] confined between the same hydrophobic walls (26). Figure 7 shows the resulting profiles for the Oxygen density, molecular orientation, and parallel permittivity (the orthogonal permittivity could not be obtained from the fluctuations). The density profiles are not unlike those observed in the simulations of Lee, McCammon, and Rossky,[19] who used a different water model, different wall-water interaction, and a narrower slit. The symmetry $\rho(z,\theta)=\rho(z,\pi-\theta)$ no longer holds, and there is indeed a nonzero average polarization $P_z(z)=\rho(z)\mu\langle\cos\theta\rangle$ close to the walls, even with no applied external field. The permittivity profile $\epsilon_\perp(z)$ shows that the bulk permittivity of SPC water $(\epsilon\simeq65)$,[20] is approximately reached after just one molecular layer inside the fluid. It is a striking result that, despite the large dielectric discontinuity between the fluid and the sur-
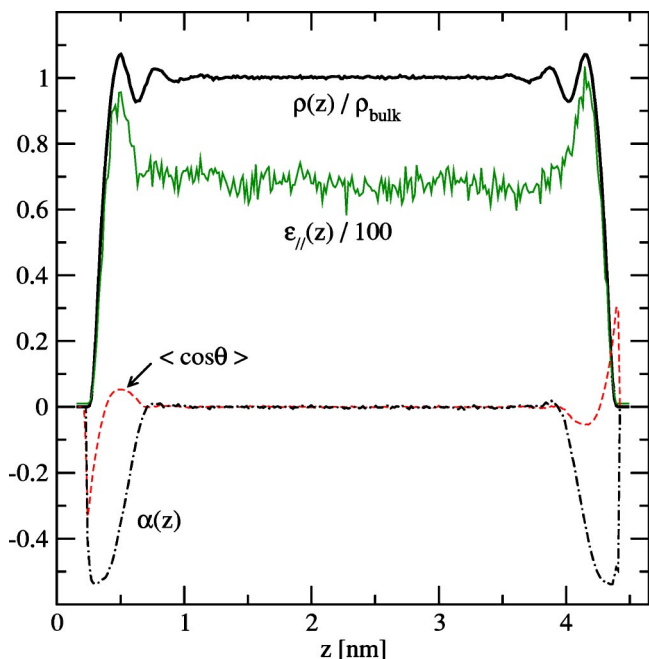
FIG. 7. Density, orientation, and permittivity profiles of 2076 SPC water molecules confined in a slab of width 4.65 nm by hydrophobic walls ($\rho_{\text{bulk}}=33.6$ nm^{-3}, $T=300$ K).
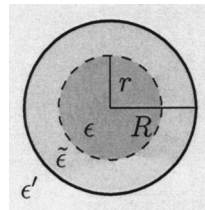
FIG. 8. Geometry for the Berendsen formula: a droplet of radius R is surrounded by a continuous medium of dielectric constant ϵ'. Dipolar fluctuations in the fluid are measured inside a concentric subsphere of radius r, while the remaining fluid in the outer shell is assumed to behave as a dielectric continuum of permittivity $\tilde{\epsilon}$.

rounding medium of dielectric constant unity, the local dipolar fluctuations in the vicinity of the interface remain almost bulklike, except in the very first layer. This behavior is in marked contrast to that observed for linear extended dipoles, illustrating the dominant influence of hydrogen bonding in the case of water.

B. Spherical geometry

The bulk dielectric constant of a spherical droplet of a polar fluid (possibly surrounded by a continuous medium of permittivity ϵ') is given in terms of dipolar fluctuations by Eq. (18). Previous workers have used another approach, which is approximate: they get the dielectric constant of a droplet from the mean square dipole $\langle m_B^2(r)\rangle$ of an inner spherical region of radius r, assuming that the remaining surrounding fluid (a shell of thickness $R-r$) can be treated as a dielectric continuum of permittivity $\tilde{\epsilon}$ (see Fig. 8). The latter approach yields the Berendsen formula,[21–23]

$$(\epsilon-1)\frac{(2\epsilon'+\tilde{\epsilon})(2\tilde{\epsilon}+1)-2(r/R)^3(\epsilon'-\tilde{\epsilon})(1-\tilde{\epsilon})}{(2\epsilon'+\tilde{\epsilon})(2\tilde{\epsilon}+\epsilon)-2(r/R)^3(\epsilon'-\tilde{\epsilon})(\epsilon-\tilde{\epsilon})}$$
$$=\frac{4\pi\beta\langle m_B^2(r)\rangle}{3V_r}, \qquad (33)$$

when $V_r=4\pi r^3/3$. Equation (33) reduces to the KF formula if $\tilde{\epsilon}=\epsilon'$ or if $r=R$. When $\tilde{\epsilon}=\epsilon$, it interpolates between the KF formula for a sphere surrounded by a medium of permittivity ϵ (for $r\ll R$), and the KF formula for a sphere surrounded by a medium ϵ' (for $r=R$).

We compared the predictions of Eq. (18) with those of Eq. (33) [with $\tilde{\epsilon}=\epsilon$], for a dipolar soft sphere fluid with parameters $\mu^*=2$, $T^*=1.35$, and $\rho_{\text{bulk}}^*=0.2$. The fluid was confined to a spherical region by external forces deriving from the potential,

$$V_R(r)=4u\sigma^9\pi\left(\frac{1}{360}\frac{1}{r}\left[\frac{9R-r}{(R-r)^9}-\frac{9R+r}{(R+r)^9}\right]-\frac{4}{9R^9}\right),$$
$$(34)$$

which arise from integrating the soft-phere repulsion potential (25) over the region $r>R$, assuming a confining medium of density $\rho_{\text{wall}}\sigma^3=1$. The results of a 30 ns long MD simulation of a droplet of $N=1000$ molecules confined in a sphere of radius $R=11.4\sigma$ surrounded by vacuum ($\epsilon'=1$) are shown in Fig. 9. Interactions were computed without the introduction of any cutoff. The estimate for ϵ based on Eq. (18)
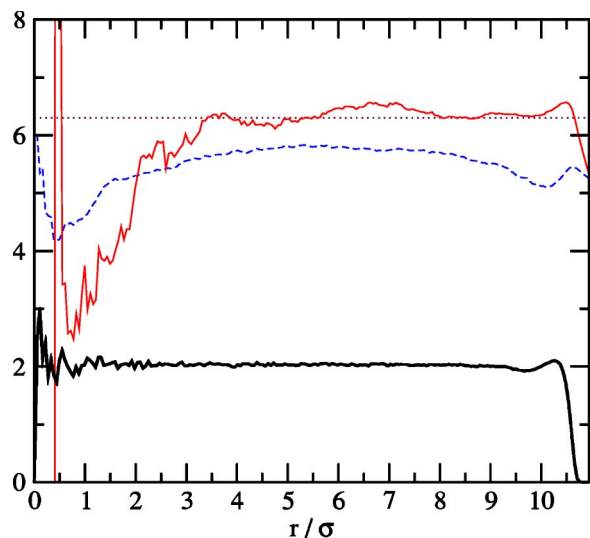
FIG. 9. Density profile [thick curve: ten times $\rho(r)\sigma^3$] and estimate of the *bulk* dielectric constant of a droplet of a polar fluid from Eq. (18) with $\mathbf{m}(\mathbf{r})$ the total dipole moment of a concentric subsphere of radius r (thin curve), and from the Berendsen formula (33) (dashed line). The expected bulk value is indicated by the dotted line.

FIG. 10. Radial electric field, polarization density, molecular density, and permittivity profiles for a spherical droplet of polar fluid ($\mu^*=2$, $T^*=1.35$, $\rho^*_{bulk}=0.2$) when an ion of unit electronic charge (reduced charge $q^*=28.7$) is present at the origin. The dotted line indicates the bulk dielectric constant $\epsilon=6.3$ (divided by 10).

agrees very well with the bulk dielectric constant $\epsilon=6.3\pm0.2$ obtained from a simulation performed under periodic boundary conditions using Ewald sums. The Berendsen approximation is seen to underestimate the dielectric constant by about 8%. It yields the most accurate estimate when r is large enough to encompass the structural angular correlations, but small compared to R so that the outer shell of the fluid can screen effectively the dipolar fluctuations. This is in contrast with Eq. (18), which provides in principle an estimate for ϵ that is independent of the chosen radius r of the inner subsphere, as long as it is small enough for boundary effects to be negligible. The variations of the estimate observed in Fig. 9, especially at small r, are to be attributed to statistical uncertainties. Notice that when $\epsilon'=1$, Eq. (18) involves the unfavorable ratio $(\epsilon-1)/(\epsilon+2)$, so that uncertainties are greatly enhanced in this case. Better estimates for the dielectric constant would be obtained by surrounding the droplet with a medium of permittivity $\epsilon'=\epsilon$, or even $\epsilon'=\infty$ (metallic boundary conditions), similarly to the case of periodically repeated systems (see discussion in Ref. 12).

We turn now to the radial dielectric permittivity profile $\epsilon(r)$ of the spherical droplet, which is defined formally by Eq. (22). The profiles for the average electric field, polarization density, molecular density, and radial permittivity are shown in Fig. 10. These results were obtained from a 35 ns long MD simulation of the previous droplet, when an ion of reduced charge $q^*=q\mu/\sigma^2 u=28.7$ is present at the origin. The total charge enclosed in a sphere a radius r around the central ion is $q(r)=q-4\pi r^2 P(r)$, since the induced charge density is $-\nabla\cdot\mathbf{P}(\mathbf{r})$. The polarization, and hence also the electric field profile $E(r)=q(r)/r^2$, can be measured directly in the simulation from the average radial polarization density $P(r)=\langle\mathbf{m}(\mathbf{r})\cdot\hat{\mathbf{r}}\rangle$. A better method, however, is to compute the profiles from the measured charge $q(r)$ enclosed in a sphere of radius r, as this yields smoother profiles thanks to the integration over the sphere.
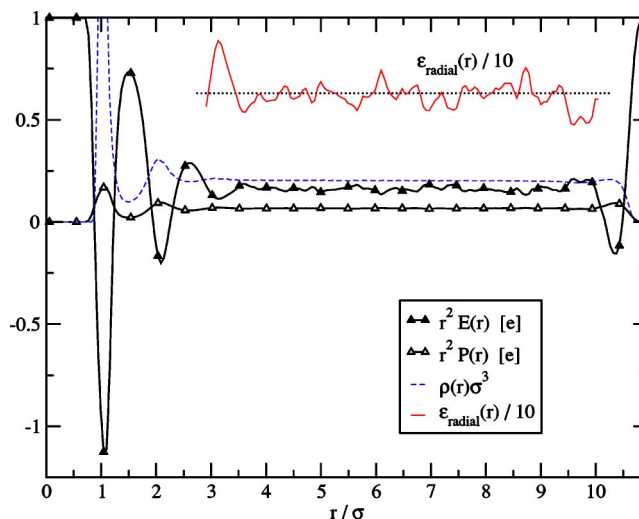
The electric field oscillates strongly close to the central ion. Overscreening of the ion's charge occurs in the first molecular layers, similarly to the behavior observed near a planar interface (Fig. 5). At distances $3\sigma<r<R$, the electric field and polarization density decay as $1/r^2$, as required by macroscopic electrostatics. The radial permittivity profile, obtained from the ratio $P(r)/E(r)$, shows qualitatively the same behavior than the orthogonal permittivity close to a planar interface: it reduces to the bulk dielectric constant far from the interfaces (here $\epsilon_{bulk}\simeq6.3$), while it is ill defined close to the central ion and close to the surface of the droplet since it diverges whenever $E(r)$ changes sign.

IV. CONCLUSION

We have combined linear response theory with extensive molecular dynamics simulations of a simple model for dipolar molecules, in an attempt to validate the concept of a local dielectric permittivity of a confined (inhomogeneous) polar fluid. The geometries which were specifically investigated correspond to a polar fluid confined between two parallel walls (slit geometry), and in a spherical cavity surrounded by a dielectric continuum. Rather large samples (thousands of polar molecules) were considered, with confinement lengths on the scale of a few nanometers, while statistics were gathered over tens of nanoseconds. The key findings of our work are the following.

(a) There is excellent agreement between the results for the permittivity tensor $\epsilon(\mathbf{r})$ obtained from the zero field fluctuation formulas derived in Sec. II, and from the explicit response of the system to an external field. Simulation results based on the latter method converge generally faster if the amplitude of the applied field is large enough. The efficiency of both methods is comparable when we take into account the computational cost of ensuring that the applied field results are not affected by nonlinearity.[24]

(b) The purely local assumption is found, perhaps not surprisingly, to break down in the vicinity of an interface. In the case of the slit geometry, the parallel component $\epsilon_\parallel(z)$ of the dielectric tensor is found to oscillate strongly, mirroring the oscillatory density profile. Contrary to a wide-spread belief, the coarse-grained envelope of $\epsilon_\parallel(z)$ tends, if anything, to increase rather than to decrease near the dielectric interfaces. This trend is observed both for dipolar soft spheres and for the SPC model of water. The tendency is opposite of that recently observed in water close to mica surfaces,[25] but in those experiments, the mica surface is highly charged, leading to local electric fields on the order of 0.2 V/nm, a strength at which nonlinear effects cannot be neglected. The orthogonal component $\epsilon_\perp(z)$ is subject to very large statistical fluctuations. It tends to take unphysical (negative) values close to the interfaces, illustrating the necessity of considering a nonlocal relation between the local polarization and the local electric field. However both $\epsilon_\perp(z)$ and $\epsilon_\parallel(z)$ go over to the bulk values beyond a few molecular diameters from the surfaces. Similar conclusions hold in spherical geometry.

(c) The fluctuation formula (18), which is closely related to the classic Kirkwood–Fröhlich formula, is an exact result that can be used to compute the bulk dielectric constant of a homogeneous spherical drop of a polar fluid. It yields an estimate of ϵ that is in better agreement with the results from simulations performed under periodic boundary conditions, than the traditional route based on the approximate Berendsen formula. For highly polar fluids, metallic boundary conditions should be used to minimize the propagation of statistical errors when solving Eq. (18) for the dielectric constant.

(d) If the local electric field $\mathbf{E}(\mathbf{r})$ varies on molecular scales, a local $\epsilon(\mathbf{r})$ may always be formally defined from the ratio of $\mathbf{P}(\mathbf{r})$ over $\mathbf{E}(\mathbf{r})$, but the resulting $\epsilon(\mathbf{r})$ then generally depends on the particular interface under consideration.

(e) In the case of a uniform external field $\mathbf{E}'$, the ratio $\mathbf{E}(\mathbf{r})/\mathbf{E}'$ is a more informative quantity, which can be computed from dipolar fluctuations [see Eq. (32)]. Our simulations point to a dramatic and unexpected "overscreening" of the applied field in the vicinity of the interfaces, which is reminiscent of overscreening of surface charges by electric double layers in highly correlated ionic systems.[26]

The main message is that the use of local permittivities in "implicit solvent" models of biomolecular aggregates is highly questionable on the nanometer scale. Future work will consider the dielectric response of polar fluids near charged (rather than hydrophobic) surfaces, and will examine the influence of the molecular graniness and the polarizability of the interface on dielectric properties of the adjacent polar fluid.

APPENDIX: EWALD SUMS IN THE SLAB GEOMETRY

There exist several exact methods for computing electrostatic interactions in systems periodic in two dimensions (2D), but most are only slowly convergent: 2D Ewald sums and the Lekner method both have an $\mathcal{O}(N^2)$ scaling, while the MMM2D method scales as $\mathcal{O}(N^{5/3})$.[27,28] A faster method is to use an efficient implementation of the full 3D Ewald

summations, leaving empty space in the simulation box outside the slab, in an attempt to decouple the interactions between the original slab and its periodic images in the z direction.[29] Adopting this approach, Yeh and Berkowitz showed that the interactions with the periodic images (in all three dimensions) must not be summed with the usual spherical convention, but rather in a slabwise manner.[30] The effect of this change in summation order is simply to replace the boundary term $U_{\text{sphere}}(\mathbf{M}) = 2\pi\mathbf{M}^2/(1+2\widetilde{\epsilon})V$ by $U_{\text{slab}}(\mathbf{M}) = 2\pi\mathbf{M}_z^2$ in the Coulomb energy, where $\widetilde{\epsilon}$ is the dielectric constant at infinity (not be be confused with the $\widetilde{\epsilon}$ introduced in Sec. III B). This simple result can be seen as a particular case of the general formula

$$U_{\text{ellipsoid}}(\mathbf{M}) = \sum_{\alpha=x,y,z} \frac{B_\alpha}{\widetilde{\epsilon}+(1-\widetilde{\epsilon})B_\alpha}\frac{2\pi M_\alpha^2}{V} \qquad (A1)$$

for the boundary term when the Coulombic interactions are summed with ellipsoidal summation order. In Eq. (A1), which is a generalization to arbitrary values of the dielectric constant $\widetilde{\epsilon}$ at infinity of a result due to Smith,[31] the dimensionless coefficients B_α are related to the semiaxes a_x, a_y, a_z of the ellipsoid by

$$B_\alpha = \frac{a_x a_y a_z}{2}\int_0^\infty \frac{1}{x+a_\alpha^2}\frac{1}{[(x+a_x^2)(x+a_y^2)(x+a_z^2)]^{1/2}}\mathrm{d}x. \qquad (A2)$$

These numbers satisfy $B_x+B_y+B_z=1$. By symmetry, $B_x=B_y=B_z=1/3$ in the case of a sphere; $B_x=B_y=1/2$, $B_z=0$ in the case of a cylinder ($a_z\to\infty$); and $B_x=B_y=0$, $B_z=1$ in the case of a slab (a_x, $a_y\to\infty$). Expression (A1) is simply the interaction energy of the charges with the depolarizing field produced by the uniform polarization density $\mathbf{M}/V$ of the infinite ellipsoidal collection of cells, when the latter is surrounded by a medium of dielectric constant $\widetilde{\epsilon}$ (see Ref. 32 for the formula of the depolarizing field in a uniformly polarized ellipsoid). In the particular case of a slabwise summation order ($B_x=B_y=0$, $B_z=1$), expression (A1) becomes independent of the permittivity $\widetilde{\epsilon}$ at infinity, as had been suspected by J de Joannis, Arnold, and Holm.[33] In the latter reference, explicit formulas to correct for the unwanted interlayer interactions in the 3D Ewald sums have been obtained, making the present approach exact in principle, while preserving its $\mathcal{O}(N\ln N)$ complexity.

Our simulation cell contained an interlayer gap of width $2L$, so that it was a parallelipiped of sides $L\times L\times 3L$. No correction term for substracting interlayer interactions was used, apart from the slabwise summation order. The Ewald sums were computed using the smooth particle mesh Ewald method (Ewald coefficient $\alpha=3.4705$ nm^{-1}, grid size $13\times 13\times 40$ cells, interpolation order 6).[34] The interactions were truncatd beyond 0.9 mm, both in the real space Ewald sum and in the soft-sphere interactions. Assuming that the forces computed using a gap of width $10L$ are the exact answers, a gap a width $2L$ leads to a relative rms error in the forces of the order of 10^{-6} for the system simulated in Sec. III A (polar fluid with $\mu^*=2$, $\rho^*_{\text{bulk}}=0.8$, confined to a slit of width 16.6σ).

[1] J. D. Jackson, *Classical Electrodynamics*, 3rd ed. (Wiley, New York, 1998)

[2] G. Nienhuis and J. M. Deutch, J. Chem. Phys. **55**, 4213 (1971).

[3] V. Ballenegger and J. P. Hansen, Europhys. Lett. **63**, 381 (2003).

[4] For a recent illustration, see, e.g., B. Mallik, A. Masunov, and T. Lazaridis, J. Comput. Chem. **23**, 1090 (2002).

[5] For a recent example, see, e.g., R. J. Allen, J. P. Hansen, and S. Melchionna, J. Chem. Phys. **119**, 3905 (2003).

[6] J. Kirkwood, J. Chem. Phys. **7**, 911 (1939).

[7] H. Fröhlich, *Theory of Dielectrics* (Clarendon, Oxford, 1949).

[8] H. A. Stern and S. E. Feller, J. Chem. Phys. **118**, 3401 (2003).

[9] M. Neumann, Mol. Phys. **50**, 841 (1983).

[10] J. G. Powles, M. L. Williams, and W. A. B. Evans, J. Phys. C **21**, 1639 (1988).

[11] T. Simonson and C. L. Brooks III, J. Am. Chem. Soc. **118**, 8452 (1996).

[12] V. Ballenegger and J. P. Hansen, Mol. Phys. **102**, 599 (2004).

[13] E. Lindahl, B. Hess, and D. van der Spoel, J. Mol. Model. [Electronic Publication] **7**, 306 (2001), http://www.gromacs.org

[14] P. G. Kusalik, M. E. Mandy, and I. M. Svishchev, J. Chem. Phys. **100**, 7654 (1994).

[15] R. J. Allen and J. P. Hansen, Mol. Phys. **101**, 1575 (2003).

[16] J. P. Badiali, J. Chem. Phys. **90**, 4401 (1989).

[17] R. Finken, V. Ballenegger, and J. P. Hansen, Mol. Phys. **101**, 2559 (2003).

[18] G. W. Robinson, S. B. Zhu, S. Singh, and M. W. Evans, *Water in Biology, Chemistry and Physics: Experimental Overviews and Computational Methodologies* (World Scientific, Singapore, 1996).

[19] C. Y. Lee, J. A. McCammon, and P. J. Rossky, J. Chem. Phys. **80**, 4448 (1984).

[20] P. Höchtl, S. Boresch, W. Bitomsky, and O. Steinhauser, J. Chem. Phys. **109**, 4927 (1998).

[21] H. J. C. Berendsen, CECAM Report No. 29, 1972 (unpublished).

[22] D. J. Adams and I. R. McDonald, Mol. Phys. **32**, 931 (1976).

[23] J. G. Powles, R. F. Fowler, and W. A. B. Evans, Chem. Phys. Lett. **107**, 280 (1984).

[24] Z. Wang, C. Holm, and H. W. Müller, J. Chem. Phys. **119**, 379 (2003).

[25] O. Teschke, G. Ceotto, and E. F. de Souza, Phys. Chem. Chem. Phys. **3**, 3761 (2001).

[26] J. P. Hansen and H. Löwen, Annu. Rev. Phys. Chem. **51**, 209 (2000).

[27] J. J. Weis and D. Levesque, J. Phys.: Condens. Matter (submitted).

[28] A. Arnold and Ch. Holm, Comput. Phys. Commun. **148**, 327 (2002).

[29] E. Spohr, J. Chem. Phys. **107**, 6342 (1997).

[30] L. C. Yeh and M. L. Berkowitz, J. Chem. Phys. **111**, 3155 (1999).

[31] E. R. Smith, Proc. R. Soc. London, Ser. A London, Ser. A **375**, 475 (1981).

[32] C. J. F. Böttcher, *Theory of Electric Polarization*, 2nd ed. (Elsevier, New York, 1973).

[33] J. de Joannis, A. Arnold, and C. Holm, J. Chem. Phys. **117**, 2496 (2002).

[34] U. Essman, L. Perela, M. L. Berkowitz, T. Darden, H. Lee, and L. G. Pedersen, J. Chem. Phys. **103**, 8577 (1995).